 doi:10.20944/preprints202006.0014.v1

Article

Multiresponsive Hybrid Microparticles for Stimuli-Responsive Delivery of Bioactive Compounds

Sergei S. Vlasov [2*], Pavel S. Postnikov [1,3], Mikhail V. Belousov [1,2], Sergei V. Krivoschekov [2], Mekhman. S. Yusubov [1,2], Artem M. Guryev [2] and Antonio Di Martino[1]

[1] Research School of Chemistry & Applied Biomedical Sciences, Tomsk Polytechnic University, Lenin Av. 30, 634050, Tomsk, Russian Federation

[2] Siberian State Medical University (SibSMU) 634050, 2 Moskovkiy trakt, Tomsk, Russian Federation

[3] Department of Solid State Engineering, University of Chemistry and Technology, 16628 Prague, Czech Republic

*Corresponding author: krivoshchekov.sv@ssmu.ru

Abstract: Hybrid microparticles based on an iron core and amphiphilic shell have been prepared to respond simultaneously to external (magnetic and ultrasounds field) and internal (pH) stimuli for delivery of the anticancer drug doxorubicin. The microparticles have been prepared in three main steps; including surface modification of the iron core followed by conjugation with the amphiphilic chitosan and drug loading. The particles demonstrate spherical shape and dimension in the range 1-3 μm with tunable surface charge by changing the pH of surrounding environment. The microparticles demonstrate good stability in simulated physiological solutions and able to allocate up to 400 μg of drug per mg of bare carrier. The response to ultrasound and the changes in the shell structure when exposed to different pH allows to control the doxorubicin release. *In vitro* cytotoxicity tests performed on fibloblast NIH/3T3 demonstrate a reduction in the cell viability when doxorubicin was administrated by microparticles compared to the free formulation; in particular when ultrasound were applied. The bare microparticles demonstrate cytocompatibility and hemocompatibility up to 50μg/mL and 60 μg/mL, respectively.

Keywords: Core-shell microparticles; ultrasound; amphiphilic polymer; magnetic microparticles; doxorubicin,

Chemical compounds studied in this article: Chitosan (CID: 71853); Iron (III) chloride Oxide (CID: 24380); Doxorubicin hydrochloride (CID: 443939); L-Lactic acid (CID: 107689)

1.Introduction

The use of stimuli-responsive or "smart" materials represents one of the most promising approaches in drug delivery to improve the pharmacokinetics parameters of active pharmaceutical ingredients (API) [1, 2]. The use of stimuli responsive materials, to develop carriers for drug delivery have found particular interest in cancer therapy, by taking advantages from the variation in the tumoral environment compared to he healthy one,e.g. lowered interstitial pH [3], high intracellular concentration of glutathione [4,5], different enzymes expression [6, 7] which can be used as triggers. Besides the physiological triggers, the use external stimuli can also be applied to stimulate and control the release of the payload from the carrier. In cancer therapy, ultrasound and magnetic field are the most attractive.Their applications can increase the temperature locally facilitating an "on-demand" drug release from the carrier but also acting on the tumor cells causing the death by hypertermia [8]. Combination of organic and inorgainc materials seem to be a promising choice in the development of hybrid carriers able to respond simultaneously to physical, chemical or biological stimuli and provide a release profile suitable for the API to improve therapeutic efficacy and reduce side effects.

Hybrid systems with a core-shell structure, where the core is inorganic and the shell organic have gained a great interest as carrier [9]. Iron metal and iron oxide-based particles are good candidate for developping hybrid material as they have been largely investigated in biomedical field

Preprints (www.preprints.org) | NOT PEER-REVIEWED | Posted: 3 June 2020 doi:10.20944/preprints202006.0014.v1

as delivery systems, contrast agents for imaging and hyperthermia [10-12]. However, the main drawback is related to the low stability with tendency to form large aggregates. To overcome it, several strategies have been reported, in particular dealing with the surface modification by introduction of specific functional groups like amino, hydroxy and carboxylic. Coating using polymers represent another most used approach as it provide a steric barrier improving the colloidal stability and prevent the agglomeration [13, 14]. The properties of the resulting carrier depends on the nature of the coating agent such as chemical structure (e.g., hydrophilicity/hydrophobicity and biodegradation characteristics), molecular weight and how it is anchored or attached (e.g., electrostatic or covalent bonding) [15].

To develop core shell carriers, with inorganic core and organic shell, both natural and synthetic polymers have been considered [16], and among those, polysaccharides have received considerable attention due peculiarities like biodegradability, biocompatibility, low toxicity and presence of different fucntional groups which allow chemical modification [17].

Among the polysaccharides, chitosan has received great attention due to the high versatility due to its chemical structure. Chitosan is made of D-glucosamino and N-Acetyl D glucosamine units. The two hydroxyl groups in C3 and C6 position, and the amino group in the deacetylated glucosamin unit represent the active sites for further conjugation with inorganic core, therapeutics, targeting ligands and imaging agents.

Herein we developed an amphiphilic derivative of chitosan by conjugation with polylactic acid. The conjugate has been used as shell for an iron core to hold either hydrophilic or hydrophobic compounds. The main aim was to load and control the release rate and intensity of a chemotherapeutic drug by application of external stimuli: magnetic field to track and ultrasounds to burst the release at a specific time and space.

In this work, doxorubicin (DOX) has been considered as a model drug. It is an anthracycline antibiotic and, it is currently used in the treatment of various cancers, including leukemia, breast cancer, ovarian cancer, and lymphomas. Besides the therapeutic efficacy, DOX exhibits severe side effects, such as cardiotoxicity, related to the low selectivity. Also, multidrug resistance usually develops, preventing further therapy with DOX. Therefore, considerable attention has been paid in the development of suitable carriers with the defined design able to improve the efficacy of DOX, which would maximize the therapeutic value while minimizing any side effects [12, 18].

As a result, the described method of preparation and modification (via arene diazonium tosylate with the addition of the amphiphilic coat) of iron microparticles allows preparing stimuli-responsive drug carriers with high stability, drug loading capacity and the possibility to control the release rate. The use of the carrier improved the DOX cytotoxicity compared to the free formulation with a decrease in the required dosage.

2. Materials and Methods

2.1. Materials

The following reagents were supplied by Sigma Aldrich: low-molecular-weight chitosan (CS), (M_w < 10^4 g/mol, D.D 75-85%); *N*-Hydroxysuccinimide (NHS); N-(3-Dimethylaminopropyl)-N'-Ethylcarbodiimide hydrochloride (EDC), commercial grade, powder; methanesulphonic acid (MSA), N,N-Dimethylformamide 99%; *tert*-Butyl nitrite, 4-toluenesulphonic acid (p-TsOH); 4-aminobenzoic acid, iron trichloride ($FeCl_3$); sodium borohydride; and doxorubicin hydrochloride. $C_3H_6O_3$ L-Lactic acid, 80% water solution, was purchased from Lachner Neratovice, Czech Republic. Sodium chloride, potassium dihydrogen phosphate, sodium carbonate, and sodium hydroxide were acquired from Penta, Prague, Czech Republic. The C_3H_6O solvent acetone, sodium hydroxide, sodium chloride, sodium phosphate, and potassium phosphate were bought from IPL Lukes, Uhresky Brod, Czech Republic. Chloroform $CHCl_3$ (HPLC grade), acetic acid CH_3CO_2H (HPLC grade), and hydrochloric acid were purchased from Chromservis, Prague, Czech Republic.

2.2. Synthesis of amphiphilic chitosan derivative

Preprints (www.preprints.org) | NOT PEER-REVIEWED | Posted: 3 June 2020 doi:10.20944/preprints202006.0014.v1

The amphiphilic polymer (PLACA-g-CS) has been obtained by grafting carboxy enrich low molecular weight polylactic acid (Mw 10 kDa) to the CS backbone by conjugation between amino and carboxylic groups. The carboxy enriched polylactic acid (PLACA) has been synthesized as described previously [19] (Di Martino & Sedlarik, 2014). The amphiphilic chitosan (PLACA-CS) has been prepared as follow; 0.5 g of CS was soaked in dimethylformamide overnight and then dissolved in 1% v/v acetic acid aqueous solution to obtain the final concentration of 2 mg/mL Afterwards, 0.5 g of PLACA (Mw 10000 g/mol), EDC and N-hydroxysuccinimide (NHS) (at the molar ratio of PLACA : EDC : NHS = 1:1.5:3) was dissolved in 50 mL of chloroform, then the solution was added to the CS and kept under vigorous stirring for 48 h at room temperature. The reaction was stopped, and the final product precipitated by adding NaOH 0.1 M and then recovered by centrifugation at 14 000 rpm for 20 minutes. The pellet was washed with chloroform, water (containing 1% v/v of acetic acid) to remove any unreacted components, and then freeze-dried.

The ^{1}H-NMR analysis was carried out to prove that grafting had taken place. Spectra were recorded on a Varian Unity Inova 400 MHz unit, using deuterium oxide supplemented with 5 % deuterium hydrochloric acid and 1 μL $(CH_3)_3COD$ for signal referencing (δ 1.23 ppm). The spectra were evaluated using 1st order spectral analysis. ^{1}H-NMR spectra are reported in the supplementary material section.

The degree of deacetylation and the number of free amino groups in the PLACA-g-CS conjugate were determined by conductometric titration, in adherence with a well-established procedure [20].

2.3. Preparation and surface modification of zero-valent iron microparticles

The zero-valent surface-modified iron microparticles (ZV) were prepared in two steps; i) preparation of the iron microparticles (IO) and ii) surface modification by diazonium chemistry [12,21]. In brief, $FeCl3*6H_2O$ (0,406 g, 1.5 mmol) and $NaBH_4$ (0.171 g, 4.5 mmol) was dissolved in the deionized water (10 mL). In triple-neck flask was added 5 mL of both solutions and left under stirring for 10 minutes under argon atmosphere with the formation of a dark precipitate. Further, to the reaction mixture was added simultaneously via syringe an additional 5 mL of $FeCl_3*6H_2O$ and 5 mL of $NaBH_4$ solutions for the microparticles growth. The resulting suspension was stirred 10 minutes in an argon atmosphere. Then 20 mL of the aqueous solution of 4-carboxybenzenediazonium tosylate (0.3 g) was added in the prepared suspension of microparticles in one portion and left under stirring for 40 minutes. The particles were isolated using a permanent magnet and washed with distilled water, ethanol, and acetone for reaching a clear solution above the particles. To remove the traces of solvents, microparticles were freeze-dried.

FTIR-ATR determined the presence of an organic layer (using a Nicolet iS5 FTIR Spectrometer equipped with an iD5 ATR accessory and ZnSe crystal, at resolution 4 cm^{-1}, for 64 scans).

2.4. Preparation of core-shell iron microparticles

The core-shell microparticles were prepared by bonding the amphiphilic chitosan derivative (PLACA-g-CS) to the surface of the ZV microparticles through amide bond between the free CS amino groups and the carboxyl groups onthe ZV microparticles surface by carbodiimide chemistry [12]. In brief, 4.6 mg NHS, 3.8 mg EDC, and 20 mg of iron microparticles were added in 20 mL of distilled water and left under mechanical stirring for the followed 6 h. The obtained suspension was added to 30 mL of chloroform solution containing PLACA-CS (200 mg). The mixture was left for 48h under stirring at 7500 rpm. Afterward, the particles were recovered by a magnet and accurately washed by distilled water to remove all the unreacted components and then freeze-dried. A schematic illustration of the processes is resumed in Figure 1 (A, B, C).

The new amide bond was detected by FTIR, the morphology, and dimension in solution by TEM while the size and the ζ-potential by laser diffraction (Marven Mastersizer).

2.5. Encapsulation efficiency and release studies

Preprints (www.preprints.org) | NOT PEER-REVIEWED | Posted: 3 June 2020 doi:10.20944/preprints202006.0014.v1

Following the positive results obtained in our previous work [12] where the optimal condition to get maximum encapsulation efficiency (EE) of DOX were settled, the initial concentration of the drug DOX was settled to 1 mg/mL (total volume 5mL) with a weight ratio between drug and the carrier of 1:10 and preparation pH 5.5.

A water solution containing DOX (1mg/mL) was added to aqueous solution containing the microparticles (10 mg/mL; V=5mL) of the and left under mechanical stirring for 24h. Afterward, the mixture was centrifuged at 14000 rpm for 15 minutes, and the pellet recovered and washed with distilled water. The supernatant was analyzed by UV-Vis (on a Perkins-Cary 300 Ultraviolet-Visible device), at 480 nm to determine the amount of DOX unloaded. To calculate the encapsulation efficiency, a standard curve was used and the encapsulation efficiency (EE) was calculated using the following equation:

$$EE(\%) = \frac{D_t - D_f}{D_t} \times 100 \quad (1)$$

where D_t represents the total theoretical amount of the drug added (mg/mL), while D_f equals the concentration after the encapsulation process (mg/mL).

Passive release:

The effecy of pH (3, 5 and 7.4) on the release kinetics of DOX was investigated under thermostable conditions (37 °C) and orbital shake (150 rpm, on a Stuart Incubator Orbital Shaker, type GFL 3033).

Briefly, 50 mg of sample was suspended in 50 mL of media; at predetermined time intervals, an aliquot (3 mL) was withdrawn and analysed on a UV-Vis spectrophotometer (Cary UV 300) and adsorbance at 480 nm recorded. The dissolution medium was replaced with fresh one to maintain the total volume constant. The amount of drug released ("DR") was determined by the following equation:

$$DR = \frac{D_0 - D_t}{D_0} \, x \, 100 \quad (2)$$

where $D_{(t)}$ (mg) represents the amount of drug released at time t, and $D_{(0)}$ (mg) the amount of loaded drug. All studies were conducted in triplicates.

Ultrasound triggered release:

Two sets of solutions containing nanoparticles (1 mg/mL V: 50 mL) were transferred into plastic tubes and placed into a water bath (37 °C). In the experiment, the following condition were set; US power (2W/cm^2 and 20 W/cm^2), the application time of 10 sec, and 30 sec per cycle. After each cycle and between two consecutive cycles, 3 mL of the media was withdrawn and replaced by a fresh one to maintain the total volume constant. The amount of DOX in the release media evaluated by the UV-Vis spectrophotometer, as described above.

2.6. Cytotoxicity and hemolysis assay

Cytotoxicity was determined by MTT assay using a fibroblast NIH/3T3 cell line. The cells were cultured in the medium (2.5 x 10^5 cells/mL) containing the formulation for 24, 48, and 72 hours. Culture medium without microparticles, bare microparticles, and free DOX were used as a control to evaluate the advantages of using microcarriers and in the particular core-shell system. The microparticles suspensions were prepared in cell growth medium at 50 µg/mL concentration. The cells were washed with 200 µL of PBS/well, and then by 50 µL of 1mg/mL MTT solution was added to each well. After 2h incubation, the MTT solution was removed by aspiration, and 50 µL of isopropanol was added to dissolve formazan crystals. A Tecan multi-plate reader was used to evaluate the optical density at 595 nm. Percentage of the cells viability was calculated as the ratio of mean absorbance of triplicate readings of sample wells (I_{sample}) compared to the mean absorbance of control wells ($I_{control}$) ;

Preprints (www.preprints.org) | NOT PEER-REVIEWED | Posted: 3 June 2020 doi:10.20944/preprints202006.0014.v1

$$Cell\ viability\ (\%) = \frac{I_{sample}}{I_{control}}\ x100 \quad (3)$$

The cytotoxicity, in combination with ultrasound, was evaluated. The formulations were seeded in 96-well plate containing 2.5 x 10^5 cells/mL and exposed to 1MHz ultrasound (2W/cm^2 and 20W/cm^2) using the same timing for the in vitro release studies. The evaluation after 48h and 72h was done to understand the effect of ultrasound treatment over time.

Hemocompatibility of bare microparticles was evaluated by the hemolysis assay following a reported protocol [22] (10.1016/j.jddst.2019.01.003). 1.5 mL of acid citrate dextrose (ACD) was added into 10 mL of human blood sample, afterwards to 1 mL of the treated sample 100 µL of the formulation containing particles was added (concentrations ranging from 5 µg/mL to 100 µg/mL) andincubated for 2 h at 37°C under orbital shaking.. The samples were centrifuge at 6000 rpm for 15 min to separate the plasma.The plasma portion was collected (100 µL plasma + 1 mL Na_2CO_3)and the OD value read at 450, 380, and 415 nm. The OD values obtained for the samples were compared to those of the control ones. In order to achieve 100% hemolysis, the cells were lysed using Triton X 100 (positive control), while negative control was obtained by treating them with PEG (1000 µg/mL). Each assay was performed in triplicate.

2.7. Statistical analysis

All the reported analysis were performed in triplicate and all data processed by one-way analysis of variance (ANOVA) with Tukey's multiple comparisons test in GraphPad Prism software (Version 6.04, San Diego, CA, USA). Probability values (p) of less than 0.05 were considered statistically significant

3. Results and discussions

3.1. Amphiphilic chitosan characterization

The success of the conjugation of PLACA to the CS backbone has been evaluated by H-NMR spectroscopy (Fig.1S). The relative spectra and the evaluation of free amino groups along the CS backbone after modification are reported in the supplementary material.

3.2. Microparticles characterization

In Figure 1, the effect of surface modification, the conjugation with PLACA-g-CS , and the impact of the surrounding pH on the average diameter and the ζ-potential of the microparticles in solution is resumed. At the preparation conditions (pH 5.5), the presence of organic layer slightly increases the microparticles dimension shifting from 800 nm to 1 µm, while following the coating the diameter increase 2 fold. ζ-potential following surface modification and polymer conjugation. In IO microparticles, the ζ-potential fluctuates around zero while in ZV it drops to -18mV due to the contribution of COO- groups and rise to +31mV in the core-shell at pH 5.5 due to the protonated free amino groups oriented towards the external environment.

Preprints (www.preprints.org) | NOT PEER-REVIEWED | Posted: 3 June 2020 doi:10.20944/preprints202006.0014.v1

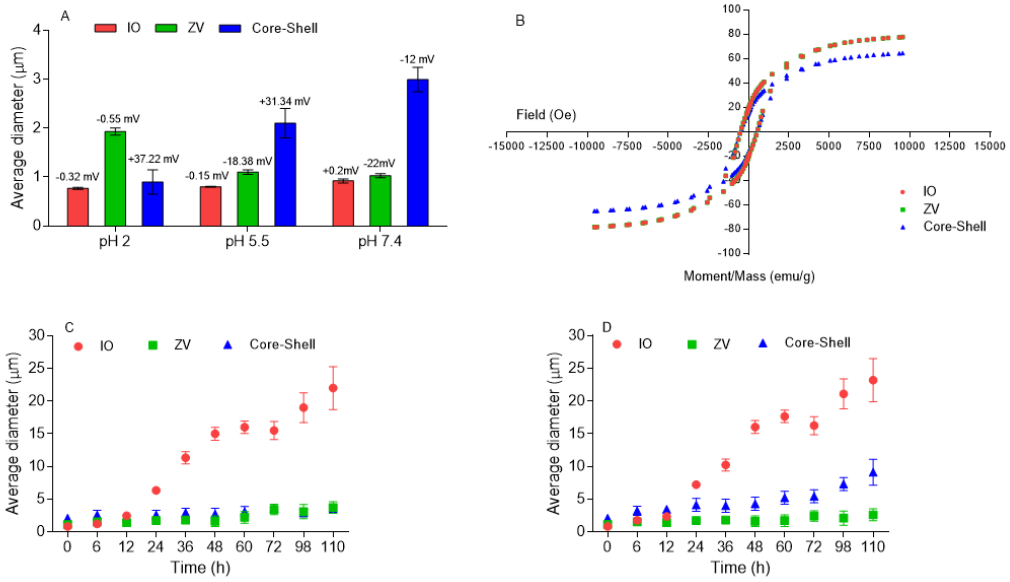

Figure 1. A) Influence of the surface modification and polymeric shell on the average diameter and ζ-potential of the microparticles in a different media; B) Magnetization curve. IO (iron oxide microparticles) has been used as a control to evaluate the effect of surface modification (ZV) and the presence of the polymeric shell (Core-Shell); C) Microparticles stability in terms of variation of average diameter versus time in C) preparation media pH 5.5 and D) physiological condition (pH7.4).

The effect of the amphiphilic shell on the magnetic properties of the microparticles was investigated by magnetometer using IO as control [12]. The saturation magnetization value (Ms) was 78 emu/g in IO and no significant variation in Ms was detected after the introduction of the organic layer. Conversely, addition of the polymer shell dropt the magnetic response up to 20% (Fig.1B). As previously described [21, 23], a Ms value of 16.3 emu/g is necessary to separate IO microparticles in aqueous solution by employing an external magnetic field [24]. With this supposition, the conditions used for preparation are optimal to preserve the magnetic response.

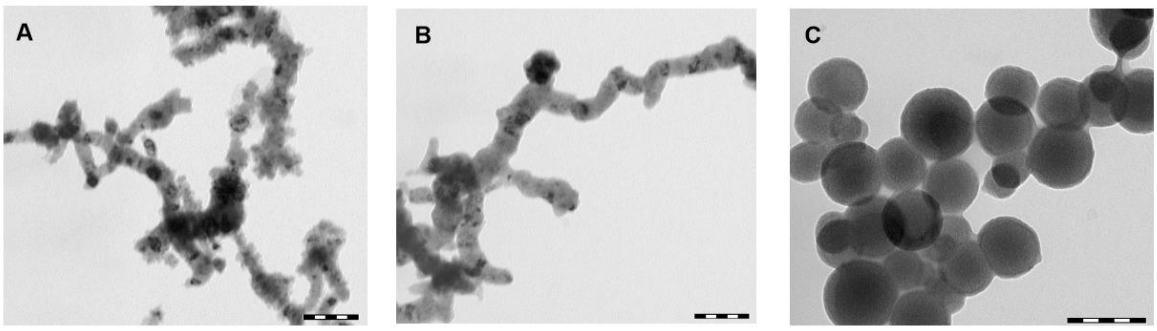

Figure 2. TEM micrograph of A) iron oxide (IO) microparticles; B) surface-modified iron oxide microparticles (ZV) and C) core-shell microparticles (Core-Shell). Scale bar is 1 µm.

As can be seen in Fig, 2A, B; IO and ZV tends to aggregate forming a string-like structure which means low stability in solution [25-27]. The TEM micrograph reported in Fig. 2B shows that addition of carboxylic groups is not enough to enhance the stability to make the microparticles suitable as carrier for drug delivery. Conversely, conjugation with the amphyphilic polymer (Fig. 2C) prevented the formation of the string structure, which can be explained by the due to the electrostatic forces, as demonstrate by the increase in ζ-potential value.

Additional proof of the success of the surface modification and polymer conjugation has been obtained by FTIR, and TGA (Thermogravimetric analysis) measurements.

Preprints (www.preprints.org) | NOT PEER-REVIEWED | Posted: 3 June 2020 doi:10.20944/preprints202006.0014.v1

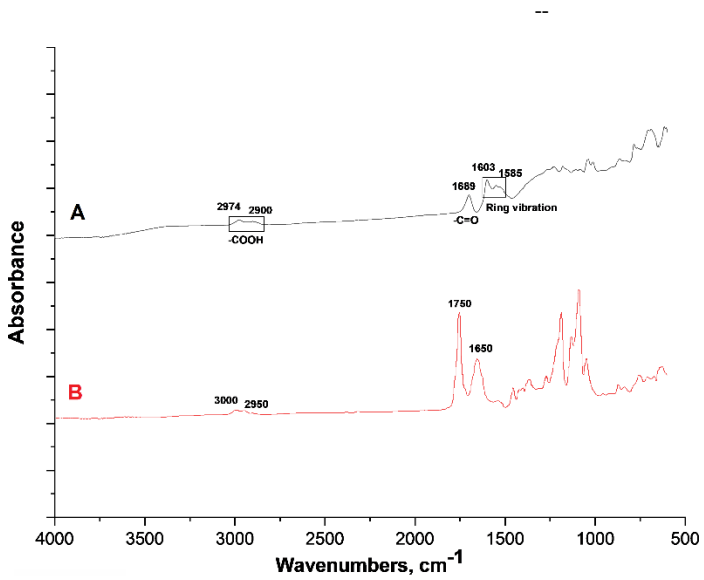

Figure 3. FTIR-ATR spectroscopy: A) Surface modified iron oxide microparticles (ZV); track B) Core-shell microparticles.

The ZV spectra (Figure 3 track **A**) peaks at 2974, 2900, 1689 cm^{-1} are ascribed to the presence of carboxylic groups while those at 1603 and 1585 cm^{-1} to the benzene ring [30]. In the spectra referring to the core-shell particles (Track B) the peaks at 3000 and 2950 cm^{-1} are related to carboxylic groups and methyl groups ($-CH_3$) in the PLACA structure. The peak at 1650 cm^{-1} might refer to the amide bonds between PLA and CS and between carboxylic groups belonging to the ZV particles and CS amino groups. The peak at 1750 cm^{-1} refers to the carbonyl group of PLACA, confirming its presence in the structure as reported previously [19]. The peaks in the range between 1000 and 1400 cm^{-1} can be attribute to the chitosan

3.3. DOX Encapsulation Efficiency

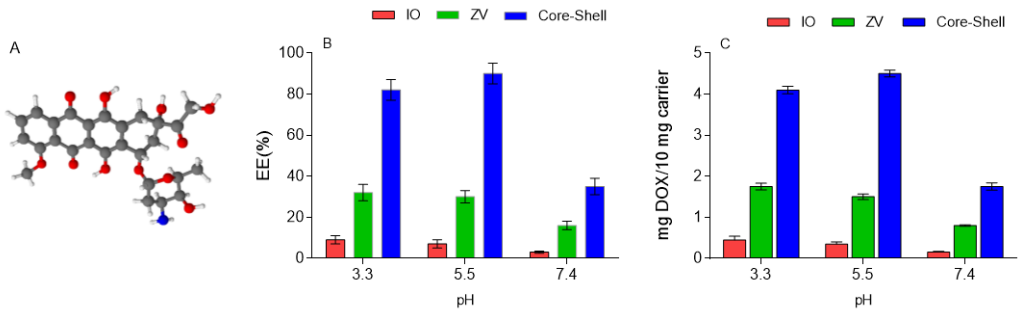

Figure 4. A) 3D structure of DOX; B) Evaluation of the effect of pH on the EE at conc.1mg/mL of drug and relationship between DOX concentration and EE at pH 5.5 (B). For encapsulation DOX conc. 1mg/mL (V = 5 mL); weight ratio between DOX and carrier is 1:10.

In the evaluation of the effect of the surface modification (ZV) and the addition of polymer shell on the DOX encapsulation efficiency, IO microparticles have been used as a control. From the data reported in Fig. 4B indicate the positive impact of the polymer coating on the ability to hold the drug with more than than 400 µg of DOX loaded in one mg of carrier. Conversely, the EE in ZV is low suggesting that DOX has been mostlyadsorbed on the surface.

Preprints (www.preprints.org) | NOT PEER-REVIEWED | Posted: 3 June 2020 doi:10.20944/preprints202006.0014.v1

3.4. Passive and US triggered DOX release kinetics

The advantages of using ultrasound as external trigger for the release is the non-invasivness, easy to regulate the depth of the penetration by tuning frequency, duty cycles, and time of exposure [28]. Additionally, it could reach deeper sites compared to light radiation and the associate sonoporation phenomenon facilitate the diffusion of therapeutic molecules through the cell membrane [29].

In vitro ultrasound-induced delivery mechanisms have been largely described [30,31]. Herein, the enhancement of DOX release after application of US cycles could be related to the oscillatory motion of the surrounded fluid occurring in the absence of cavitation. Herein, two main mechanism can be responsible to the enhancement in the DOX release following US application; the first, is due to the oscillation of the surrounding fluid which increase the diffusivity of the molecules and the second can be related to the rupture of the carrier structure.However, the former should be marginal as a complete disruption of the particles is followed by an intense burst.

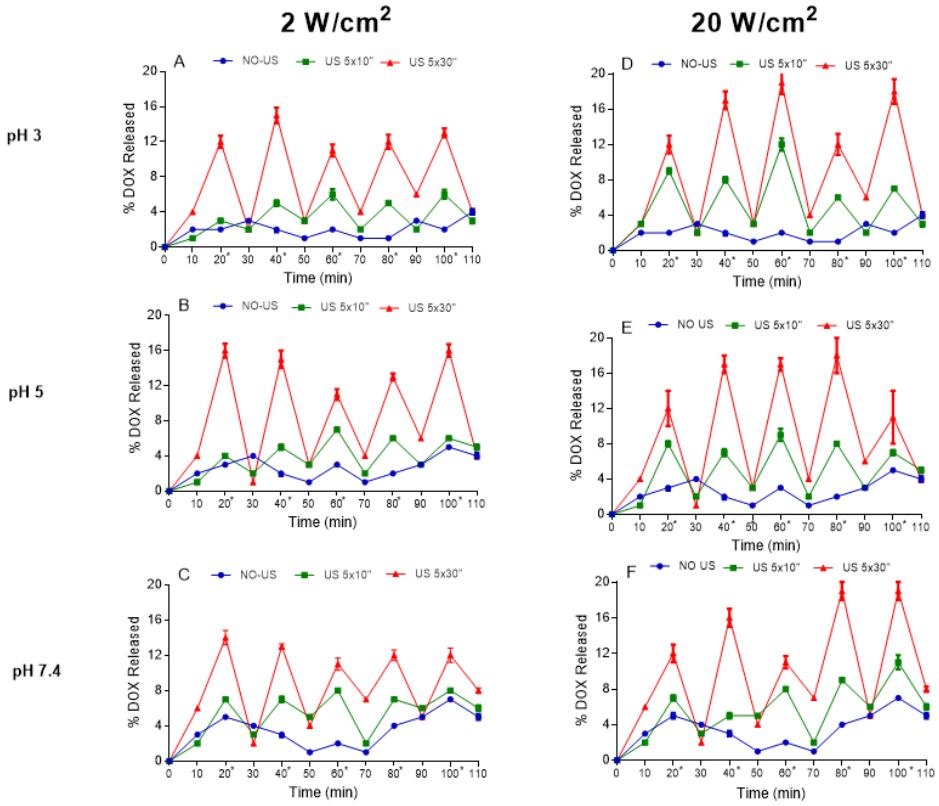

--

Figure 5. Evaluation of the effect of the US in terms of power and application time on the DOX release in different media.

The trend illustrated in Fig. 5 shows how the exposure to ultrasound triggered the release, with an increase between 10-50% with a maximum at 20 W/cm^2 power and 30 sec application.

In table 1, the amount of DOX, in mg per 10 mg of the carrier, released from core-shell microparticles is resumed. The total amount of DOX referred after 110 min per 10 mg of the carrier. In the bracket, the percentage released referred to the amount loaded is reported. It relates to 10 mg of the carrier.

Preprints (www.preprints.org) | NOT PEER-REVIEWED | Posted: 3 June 2020 doi:10.20944/preprints202006.0014.v1

Table 1. Total amount of DOX released in different media and US conditions from 10mg of the carrier. Data referred to the release trend illustrated in Fig. 5.

	Total DOX released (µg)		
2W/cm^2			
pH	NO US	US 10''	US 30''
3	1276(29%)	1892(43%)	**3828(87%)**
5.5	1452(33%)	2112(48%)	**4180(95%)**
7.4	1628(37%)	2728(62%)	**4268(97%)**
20W/cm^2			
pH	NO US	US 10''	US 30''
3	1276(29%)	2684(61%)	**4400(100%)**
5.5	1452(33%)	2552(58%)	**4268 (97%)**
7.4	1628(37%)	2816(64%)	**4312(98%)**

The data demonstrates how the burst occurs at all pH conditions under US application. In the absence of US, the amount of DOX released increases when pH moves from acidic to physiological, but in a lower intensity and the drug released is only 37% of the loaded amount in physiological condition. The application of US tends to double and triple the amount of DOX released overcoming 85% in all cases. Both tested parameters, time and power, affect the amount of DOX released. As expected, increasing exposure time and power, the amount of released DOX increases. Application of 20W/cm^2 power for 30 sec almost 100% of the loaded drug is released at any pH condition tested.

3.5. Cytotoxicity and hemolysis assessment of microparticles

The MTT has been performed to determine the i) the cytotoxicity of the bare microparticles and the impact of the surface properties in the in vitro biocompatibility; ii) the advantages of using microcarrier in the delivery of DOX compared to the free drug, in particular in the in vitro cytotoxicity enhancement; iii) DOX cytotoxicity extended overtime. IO microparticles have been used as the control to evaluate the advantages of surface modification and polymer conjugation in improving the biocompatibility of iron-based systems. NIH/3T3 cells were treated with 50 µg of microparticles, and the viability determined after 24, 48, and 72 h (Fig.6). The toxic effect was taken into consideration when the viability was below 80 %.

Preprints (www.preprints.org) | NOT PEER-REVIEWED | Posted: 3 June 2020 doi:10.20944/preprints202006.0014.v1

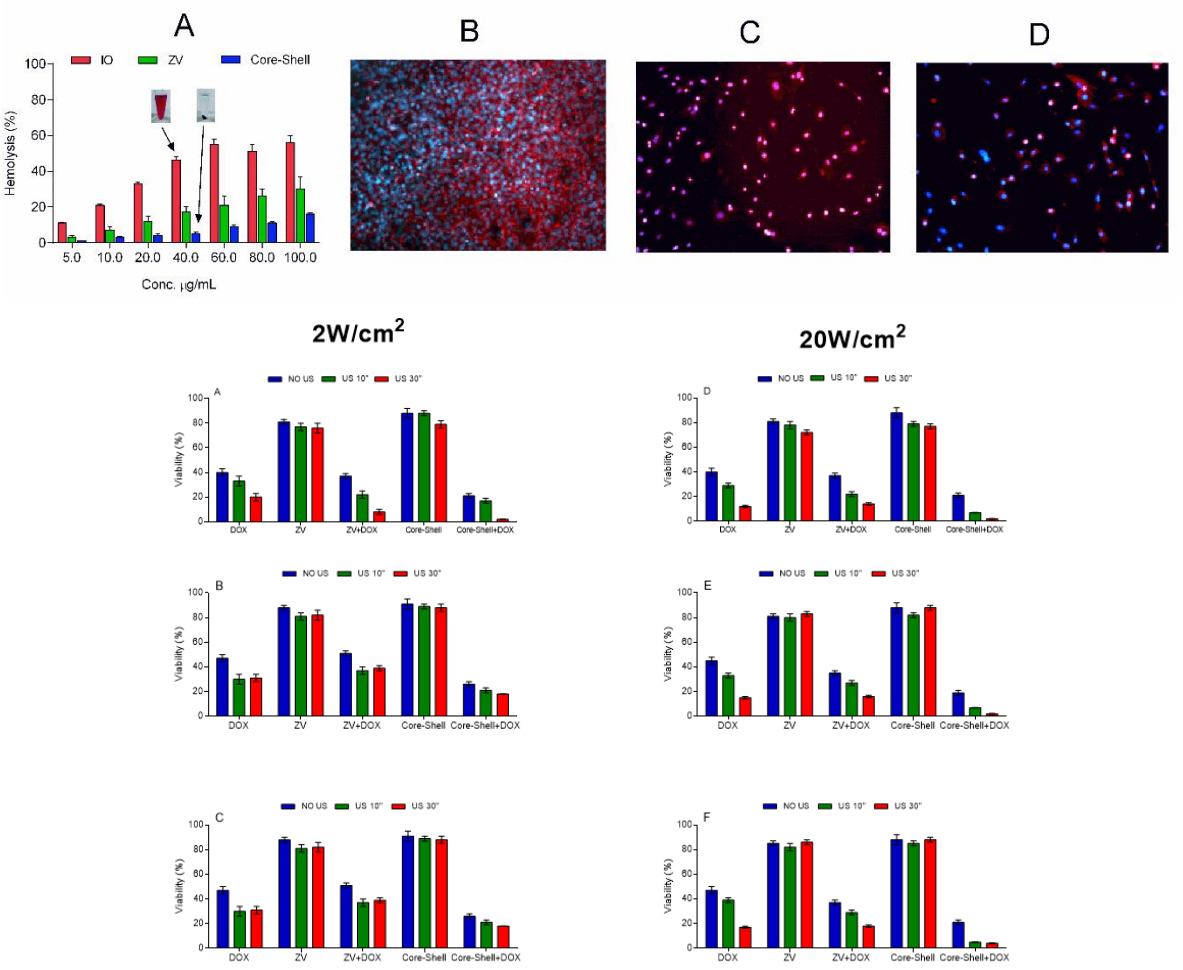

Figure 6. Cell viability evaluation for all formulations with and without application of US (concentration of particles 50 µg./mL). A,B,C) 2W/cm² and D,E,F) 20W/cm² The cells were incubated with the relative samples Core-s at concertation of 50 µg/mL, treated with 5 cycles US within 110 minutes (the timing used for the release was followed).

Results reported in Fig.6 prove the advantageous role played by the core-shell carrier in driving the drug inside the cells. According to the value, the presence of the polymer shell could play a specific role in the cell uptake and in controlling the release of the drug. In fact, DOX cytotoxicity is higher when loaded in core-shell structure than in ZV where the release begins immediately after contact with the media, leading to the release of a certain amount of the drug in the solution before the internalization of the particles The cell viability tends to decrease over time when exposed to core-shell microparticles, conversely to the free DOX that after 48 h and 72 h the viability increased, even if the value is maintained much lower in comparison.

The MTT tests were also performed in the presence of US using the same power, the number of cycles, and application time used in the release studies. The application of US at 2 and 20 W/cm² power did not affect the cell viability but might alter, reversibly, the structure of the membrane of the cell by sonoporation favoring the entry of the microparticles and free DOX. In the case of core-shell microparticles, the positive surface charge represents an additional advantage to support the interaction with the cells which have membrane negatively charged. The use of US cycles; 5x10 sec and 5x 30 sec do not cause any significant increase in temperature with a variation of less than 1 ^{0}C. It is important to define as the temperature affects the shell structure and, consequently, the release rate and mechanism. Moreover, an increase in temperature can also influence cell viability.

Preprints (www.preprints.org) | NOT PEER-REVIEWED | Posted: 3 June 2020 doi:10.20944/preprints202006.0014.v1

From the data resumed in Fig.6, cytotoxicity of free DOX and DOX-loaded ZV particles is lower than core-shell particles due to the prolonged release of the drug. As reported in the release studies, US causes a burst in the DOX release, meaning that a large amount of drug is released in a narrow range of time, and combination with the sonoporation permits a better uptake and effectivity of the drug. The increase in vitro cytotoxicity of DOX by using the US is given by the synergic effects of US and DOX. US acts either directly and indirectly, by sonoporation and bursting the DOX release. Moreover, the possibility to turn on and off the burst is only possible by using core-shell systems. In the case of ZV, it is not possible to control the burst, and the application of a single cycle of US causes an intensive burst was almost all the adsorbed drug is released. Analyzing the effect of US exposure on the cell viability it can be resumed by two factors (direct and indirect): i) improve in the microparticles permeability through the cell membrane by sonoporation (direct) as reported [32]; ii) burst the release of DOX (indirect) reaching highly concentration which results highly toxic for the cells. As can be seen from Fig. 6, in the case of bare ZV and Core-Shell microparticles and absence of US and coated with the cell viability is higher than 80 %, and it persists up to 72 h, indicating the not in vitro cytotoxicity for the selected cell lines at the tested concentration. However, due to the nature of the material used, it was expected a not cytotoxic profile. In agreement with our previous studies and others already published [33-35], cells treated with free DOX solution demonstrate viability around 40 %, confirming the well-known cytotoxicity of the drug.

Results reported in Figure 6 prove the beneficial role played by the core-shell carrier in driving the drug inside the cells. According to the value, the presence of the polymer shell could play a specific role in the cell uptake and in controlling the release of the drug. In fact, DOX cytotoxicity is higher when loaded in core-shell structure than in ZV where the release begins immediately after contact with the media, leading to the release of a certain amount of the drug in the solution before the internalization of the particles The cell viability tends to decrease over time when exposed to core-shell microparticles, conversely to the free DOX that after 48 h and 72 h the viability increased, even if the value is maintained much lower in comparison.

-

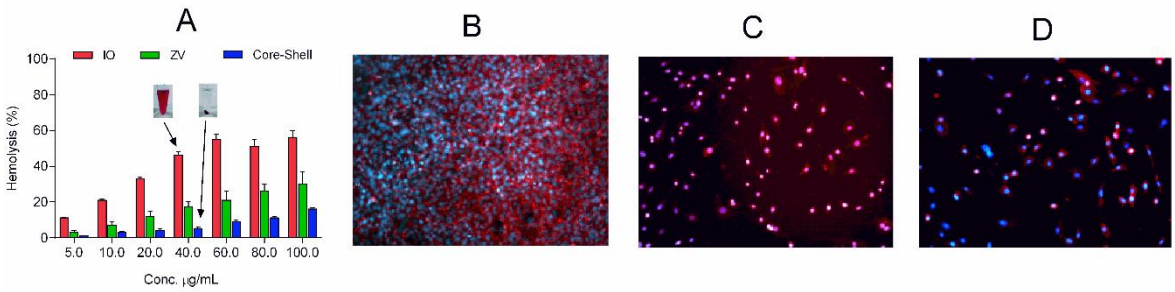

Figure 7. Effect of the surface modification on the hemolysis of the particles at different concentrations. Micrographs of NIH/3T3 cells incubated with core-shell microparticles after exposition to US treatment. The micrograph was taken after 24h exposition. 50µg/mL was the microparticles concentration used, B) control, only cells; C) cells incubated with core-shell microparticles and exposed to US treatment 2W/cm^2; D) cells incubated with core-shell microparticles and exposed to US treatment 20W/cm^2.

Blood compatibility represents a critical parameter to evaluate biological safety when materials are intended for intravenous injection. The date resumed in Figure 7 gives essential information. As can be seen, the introduction of the organic layer on IO, reduced the hemotoxicity with acceptable concentration up to 10 µg/mL. More interesting is to observe the increase in hemocompatibility after the conjugation of the amphiphilic polymer. In fact, in core-shell microparticles, the acceptable concentration raises to 60 µg/mL, 6 folds higher than ZV, indicating a further advantage of using the amphiphilic polymer.

 doi:10.20944/preprints202006.0014.v1

4. Conclusions

In the present work, hybrid core-shell microparticles with a design based on iron core and amphiphilic shell able to respond to pH, magnetic field, and ultrasounds were developed for the stimuli-responsive delivery application. As a model drug, doxorubicin has been used due to its well-known efficacy in the treatment of different cancers. The core-shell microparticles were prepared in three main steps; i) preparation of iron oxide microparticles; ii) surface modification by the introduction of phenyl carboxyl groups; iii) conjugation with the amphiphilic CS derivative (PLACA-g-CS). The core-shell microparticles shown a dimension around 3μm and positive ζ-potential, 34 mV, with excellent stability in the physiological environment.

In comparison with the iron core, the presence of the amphiphilic polymer shell allow a higher encapsulation efficiency and a pH-dependent controlled delivery. The presence of the polymer did not affect the magnetic response of the iron core under a magnetic field, with a decrease limited to 20%. The core-shell system demonstrates a US responsive behavior characterized by a reversible change in the spatial displacement of the polymeric chains around the core, causing a burst with intensity dependent on the power and application time of the US. The in vitro test performed on NIH/3T3 cells demonstrate that the use of core-shell microparticles in the combination of US improves the cytotoxicity of doxorubicin, and it lasts for a longer time compared to the free drug formulation. Moreover, the prepared hybrid system demonstrates good hemocompatibility with concentration up to 60μg/mL, 6 fold higher compared to iron oxide microparticles.

Acknowledgments

This research has been supported by the Ministry of Science and Higher Education of the Russian Federation (State Project "Science" № FSWW-2020-0011).

Conflicts of Interest: Declare conflicts of interest or state "The authors declare no conflict of interest."

References

1. Mura, S.; Nicolas, J.; Couvreur, P. Stimuli-responsive nanocarriers for drug delivery. Nature Mater. 2013, 12, 991-1003; DOI: 10.1038/nmat3776
2. Jhaveri, A.; Deshpande, P.; Torchilin, V. Stimuli-sensitive nanopreparations for combination cancer therapy. J. Control Release. 2014, 190, 352-370; DOI: 10.1016/j.jconrel.2014.05.002
3. Zhang, S.; Wu, K.; Sherry, A.D. A novel pH-sensitive MRI contrast agent. Angew. Chem. Int. Ed. 1999, 38, 3192-3194; DOI: 10.1002/(SICI)1521-3773(19991102)38:21<3192::AID-ANIE3192>3.0.CO;2-%23
4. Liu, J.; Dang, H.; Wang, X.W. The significance of intertumor and intratumor heterogeneity in liver cancer. Ex. Mol. Med. 2018, 50, 416; DOI:10.1038/emm.2017.165
5. Assenov, Y.; Brocks, D.; Gerhäuser, C. Intratumor heterogeneity in epigenetic patterns. Semin. Cancer biol. 2018, 51, 12-21; DOI: 10.1016/j.semcancer.2018.01.010.
6. De La Rica, R.; Aili, D.; Stevens, M.M. Enzyme-responsive nanoparticles for drug release and diagnostics. Adv. Drug Deliv. Rev. 2012, 64, 967-978; DOI: 10.1016/j.addr.2012.01.002
7. Jha, S.; Sharma, P.K.; Malviya, R. Hyperthermia: role and risk factor for cancer treatment. Achievements in the Life Sciences. 2016, 10, 161-167; DOI: 10.1016/j.als.2016.11.004
8. Li, Y.; Xiao, K.; Zhu, W.; Deng, W.; Lam, K.S. Stimuli-responsive cross-linked micelles for on-demand drug delivery against cancers. Adv. Drug Deliv. Rev. 2014, 66, 58-73; DOI: 10.1016/j.addr.2013.09.008

9. Bachhuka, A.; Christo, S. N.; Cavallaro, A.; Diener, K. R.; Mierczynska, A.; Smith, L. E.; Vasilev, K. Hybrid core/shell microparticles and their use for understanding biological processes. J. Colloid Interface Sci. 2015, 457, 9-17; DOI: 10.1016/j.jcis.2015.06.040

10. Oh, J.K.; Park, J.M. Iron oxide-based superparamagnetic polymeric nanomaterials: design, preparation, and biomedical application. Progress in polymer Science. 2011, 36, 168-189; DOI: 10.1016/j.progpolymsci.2010.08.005

11. Bai, M.Y.; Tang, S.L.; Chuang, M.H.; Wang, T.Y.; Hong, P.D. Evaluation of chitosan derivative microparticles encapsulating superparamagnetic Iron oxide and doxorubicin as a pH-sensitive delivery carrier in hepatic carcinoma treatment: an in vitro comparison study. Front. Pharmacol. 2018, 9, 1025; DOI:10.3389/fphar.2018.01025

12. Di Martino, A.; Guselnikova, O.A.; Trusova, M.E.; Postnikov, P.S.; Sedlarik, V. Organic-inorganic hybrid nanoparticles controlled delivery system for anticancer drugs. International journal of pharmaceutics. 2017, 526, 380-390; DOI: 10.1016/j.ijpharm.2017.04.061

13. Yuan, A.; Wu, J.; Tang, X.; Zhao, L.; Xu, F.; Hu, Y. Application of near-infrared dyes for tumor imaging, photothermal, and photodynamic therapies. Journal of pharmaceutical sciences. 2013. 102, 6-28; DOI: 10.1002/jps.23356

14. Yiyun, C.; Na, M.; Tongwen, X.; Rongqiang, F.; Xueyuan, W.; Xiaomin, W.; Longping, W. Transdermal delivery of nonsteroidal anti-inflammatory drugs mediated by polyamidoamine (PAMAM) dendrimers. J. Pharm. Sci. 2007. 96, 595-602; DOI: 10.1002/jps.20745

15. Castelló, J.; Gallardo, M.; Busquets, M.A.; Estelrich, J. Chitosan (or alginate)-coated iron oxide nanoparticles: a comparative study. Colloids Surf. A. 2015, 468, 151-158; DOI: 10.1016/j.colsurfa.2014.12.031

16. Chuah, W.H.; Zhang, W.L.; Choi, H.J.; Seo, Y. Magnetorheology of core–shell structured carbonyl iron/polystyrene foam microparticles suspension with enhanced stability. Macromolecules. 2015, 48, 7311-7319; DOI: 10.1021/acs.macromol.5b01430

17. Soares, P.I.; Machado, D.; Laia, C.; Pereira, L.C.; Coutinho, J.T.; Ferreira, I.M.; Borges, J.P. Thermal and magnetic properties of chitosan-iron oxide nanoparticles. Carbohydr. Polym. 2016, 149, 382-390; DOI: 10.1016/j.carbpol.2016.04.123

18. Abaan, O.D.; Mutlu, P.K.; Baran, Y.; Atalay, C.; Gunduz, U. Multidrug resistance mediated by MRP1 gene overexpression in breast cancer patients. Cancer Invest. 2009, 27, 201-205; DOI: 10.1080/07357900802173562

19. Di Martino, A.; Sedlarik, V. Amphiphilic chitosan-grafted-functionalized polylactic acid based nanoparticles as a delivery system for doxorubicin and temozolomide co-therapy. Int. J. Pharm. 2014, 474, 134-145; DOI: 10.1016/j.ijpharm.2014.08.014

20. Guselnikova, O.A.; Galanov, A.I.; Gutakovskii, A.K.; Postnikov, P.S. The convenient preparation of stable aryl-coated zerovalent iron nanoparticles. Beilstein journal of nanotechnology. 2015, 6, 1192-1998; DOI: 10.3762/bjnano.6.121

21. Ma, Z.; Guan, Y.; Liu, H. Synthesis and characterization of micron-sized monodisperse superparamagnetic polymer particles with amino groups. J. Polym. Sci. A. Polym. Chem. 2005, 43, 3433-3439; DOI: 10.1002/pola.20803

22. Anirudhan, T.S.; Divya, P.L.; Nima, J. Synthesis and characterization of novel drug delivery system using modified chitosan based hydrogel grafted with cyclodextrin. Chem. Eng. J. 2016, 284, 1259-1269; DOI: 10.1016/j.cej.2015.09.057

23. Chatterjee, J.; Haik, Y.; Chen, C.J. Modification and characterization of polystyrene-based magnetic microspheres and comparison with albumin-based magnetic microspheres. J. Magn. Magn. Mater. 2001, 225, 21-29; DOI: 10.1016/S0304-8853(00)01223-3

24. Hałupka-Bryl, M.; Bednarowicz, M.; Dobosz, B.; Krzyminiewski, R.; Zalewski, T.; Wereszczyńska, B.; Nagasaki, Y. Doxorubicin loaded PEG-b-poly (4-vinylbenzylphosphonate) coated magnetic iron oxide nanoparticles for targeted drug delivery. J. Magn. Magn. Mater. 2015, 384, 320-327; DOI: 10.1016/j.jmmm.2015.02.078

25. Estelrich, J.; Escribano, E.; Queralt, J.; Busquets, M.A. Iron oxide nanoparticles for magnetically-guided and magnetically-responsive drug delivery. Int. J. Mol. Sci. 2015, 16, 8070-8101; DOI: 10.3390/ijms16048070

26. Tiraferri, A.; Chen, K.L.; Sethi, R.; Elimelech, M. Reduced aggregation and sedimentation of zero-valent iron nanoparticles in the presence of guar gum. J. Colloid Interface Sci. 2008, 324, 71-79; DOI: 10.1016/j.jcis.2008.04.064

27. Chehimi, M.M.; Lamouri, A.; Picot, M.; Pinson, J. Surface modification of polymers by reduction of diazonium salts: polymethylmethacrylate as an example. J. Mater. Chem. C. 2014, 2, 356-363; DOI: 10.1039/c3tc31492h

28. Sonis, S.T. Ultrasound-mediated drug delivery. Oral diseases. 2017, 23, 135-138; DOI: 10.1111/odi.12501

29. Liu, Y.; Lillehei, K.; Cobb, W.N.; Christians, U.; Ng, K.Y. Overcoming MDR by ultrasound-induced hyperthermia and P-glycoprotein modulation. Biochem. Biophys. Res. Commun. 2001, 289, 62-68; DOI: 10.1006/bbrc.2001.5938

30. Park, J.; Aryal, M.; Vykhodtseva, N.; Zhang, Y.Z.; McDannold, N. Evaluation of permeability, doxorubicin delivery, and drug retention in a rat brain tumor model after ultrasound-induced blood-tumor barrier disruption. J. Control Release. 2017, 250, 77-85; DOI: 10.1016/j.jconrel.2016.10.011

31. Lentacker, I.; De Cock, I.; Deckers, R.; De Smedt, S.C.; Moonen, C.T.W. Understanding ultrasound induced sonoporation: definitions and underlying mechanisms. Adv. Drug Deliv. Rev. 2014, 72, 49-64; DOI: 10.1016/j.addr.2013.11.008

32. Yao, J.; Feng, J.; Chen, J. External-stimuli responsive systems for cancer theranostic. Asian J. Pharm. Sci. 2016, 11, 585-595; DOI: 10.1016/j.ajps.2016.06.001

33. Tacar, O.; Sriamornsak, P.; Dass, C.R. Doxorubicin: an update on anticancer molecular action, toxicity and novel drug delivery systems. J. Pharm. Pharmacol. 2013, 65, 157-170; DOI: 10.1111/j.2042-7158.2012.01567.x

34. Unsoy, G.; Khodadust, R.; Yalcin, S.; Mutlu, P.; Gunduz, U. Synthesis of Doxorubicin loaded magnetic chitosan nanoparticles for pH responsive targeted drug delivery. Eur. J. Pharm. Sci. 2014, 62, 243-250; DOI: 10.1016/j.ejps.2014.05.021

35. Soares, P.I.; Sousa, A.I.; Silva, J.C.; Ferreira, I.M.; Novo, C.M.; Borges, J.P. Chitosan-based nanoparticles as drug delivery systems for doxorubicin: Optimization and modelling. Carbohyd. Polym. 2016, 147, 304-312; DOI: 10.1016/j.carbpol.2016.03.028

[